MICROSTRUCTURE OF ISOTOPICALLY-TAILORED MARTENSITIC STEEL HT9 IRRADIATED AT 400°C TO 7 DPA IN HFIR - N. Hashimoto, J.P. Robertson (Oak Ridge National Laboratory), and K. Shiba (Japan Atomic Energy Research Institute)

OBJECTIVE

The objective of this work is to generate TEM data for isotopically-tailored martensitic steel HT9 irradiated in the temperature range for swelling.

SUMMARY

The microstructures of reduced-activation martensitic steel, HT9-std. (12Cr-1MoVW) and HT9 doped with ^{58}Ni and ^{60}Ni, irradiated at 400°C to 7 dpa in the High Flux Isotope Reactor (HFIR), were investigated by transmission electron microscopy. No cavities were observed in any alloys. Irradiation-induced $\mathbf{a_0}$<100> and ($\mathbf{a_0}$/2)<111> type dislocation loops were observed in all alloys; the number density and the mean diameter of $\mathbf{a_0}$<100> type loops were higher and larger than that of (a_0/2)<111> type loops. Also, there was a tendency for the number density of loops in the HT9 doped with ^{60}Ni to be lower than those in the other alloys. Irradiation-induced precipitates were observed in all alloys, which were identified as $M_6C(\eta)$ type carbide, α' phase and M_2X phase. The $M_6C(\eta)$ type carbides and α' phase were formed along dislocation loops, suggesting that dislocation loops are sites of Cr segregation during irradiation and that Cr segregation plays an important role in the precipitation behavior in martensitic steels.

PROGRESS AND STATUS

1. Introduction

Ferritic/martensitic steels are attractive candidate structural first wall materials for fusion energy systems [1]. The high-energy neutrons produced by the D-T fusion reaction induce displacement damage and generate gas atoms in the materials from (n,p) and (n,α) reactions. Simultaneous production of helium atoms from (n,α) reactions is considered to strongly influence the nucleation processes of cavities. To clarify the effect of helium atoms on the microstructural development and mechanical property change in martensitic steels under fast neutron irradiation, HT9 (12Cr-1MoVW) and HT9 doped with ^{58}Ni and ^{60}Ni were irradiated with neutrons in the High Flux Isotope Reactor (HFIR). Irradiation of ^{58}Ni-doped alloys in a mixed spectrum reactor like the HFIR results in the following transmutation reaction with the thermal neutrons: $^{58}Ni(n,\gamma)^{59}Ni(n,\alpha)^{56}Fe$. The concept of isotopic tailoring to separate the individual effects of Ni and helium on microstructural development was described earlier [2-4]. The specimens examined here are part of an experiment conceived 10 years ago by researchers at ORNL, UCSB and PNNL and irradiated under the US/JAERI collaborative irradiation program. Another part of this experiment utilizing ^{60}Ni and ^{59}Ni doping was described earlier by D.S. Gelles [5].

2. Experimental Procedure

HT9, and HT9 doped with ^{58}Ni and ^{60}Ni were included in this experiment; the compositions and heat treatment are given in Table 1. Standard 3-mm diameter transmission electron microscopy (TEM) disks were punched from 0.25-mm thick sheet stock. Irradiation was carried out at 400°C in the capsules of HFIR-MFE-JP-20 in the High Flux Isotope Reactor (HFIR) to a neutron fluence of ~ 5.16×10^{25} n/cm^2 (E> 0.1 MeV), resulting in a displacement dose of ~ 7.4 dpa. The details of the design, construction, and installation of JP-20 have been reported [6-9]. The irradiation conditions and the calculated helium concentrations in the steels are given in Table 2.

Table 1. Chemical compositions of the specimens (wt%) (Balance Fe) and heat treatment.

Steel	Cr	^{n}Ni	^{58}Ni	^{60}Ni	Si	C	N	Mn	W	V	Nb	Mo
HT9-std.	12.0	0.5	-	-	0.18	0.20	0.02	0.5	0.5	0.3	0.01	1.0
HT9-1.4wt%^{58}Ni	12.0	-	1.4	-	0.18	0.20	0.02	0.5	0.5	0.3	0.01	1.0
HT9-0.5wt%^{60}Ni	12.0	-	-	0.5	0.18	0.20	0.02	0.5	0.5	0.3	0.01	1.0
HT9-1.4wt%^{60}Ni	12.0	-	-	1.4	0.18	0.20	0.02	0.5	0.5	0.3	0.01	1.0

Heat treatment: 1050°C/1 h/ AC + 780°C/2.5 h/ AC

Table 2. Irradiation conditions and helium concentration.

	dpa	appm He	He/dpa
HT9-std.	7.4	10	1.3
HT9-1.4wt%^{58}Ni	7.4	40	5.2
HT9-0.5wt%^{60}Ni	7.4	-	-
HT9-1.4wt%^{60}Ni	7.4	-	-

TEM specimens were thinned using an automatic Tenupol electropolishing unit located in a shielded glove box. TEM disks were examined using a JEM-2000FX (LaB_6) transmission electron microscope equipped with a special objective lens polepiece that lowers the magnetic field at the ferro-magnetic specimen. The foil thicknesses were measured by thickness fringes in order to evaluate quantitative defect density values.

3. Results and discussion

3.1 Dislocations and dislocation loops

During irradiation of Fe-Cr binary alloys, dislocation evolution in an initially almost dislocation-free condition proceeds by the formation of interstitial type dislocation loops with an $\mathbf{a_0}$<100> and/or (a_0/2)<111> Burgers vector [10,11]. Figure 1 shows the dislocation segments and loops in the HT9 alloys after irradiation at 400°C to 7.4 dpa using the diffraction conditions: **g**=110, (**g**,4**g**). Table 3 summarizes the quantitative results of dislocation loops. In all of the alloys, there is a tendency for the number density of irradiation-induced $\mathbf{a_0}$<100> and (a_0/2)<111> type dislocation loops in HT9-std. and HT9 doped with ^{58}Ni to be higher than those in the HT9 doped with ^{60}Ni. This suggests that the existence of helium generated by the (n,α) reaction with the thermal neutrons assists the nucleation of dislocation loops in these alloys. On the other hand, the number density and the mean diameter of $\mathbf{a_0}$<100> type loops in all alloys are higher and larger than that of (a_0/2)<111> type loops, respectively. According to a previous paper which investigated a relationship between the type of dislocation loop and the content of interstitial impurities [12], there is a tendency for $\mathbf{a_0}$<100> type loop to form in alloys which have high concentrations carbon and nitrogen, which is true for the alloys used in this study.

Table 3. The summary of dislocation loops in alloys after irradiation at 400°C to 7.4 dpa in HFIR.

Steel	a_0<100> type loops		(a_0/2)<111> type loops	
	Number density (m^{-3})	Mean diameter (nm)	Number density (m^{-3})	Mean diameter (nm)
HT9-std.	1×10^{22}	14	3×10^{21}	10
HT9-1.4wt%^{58}Ni	1×10^{22}	16	5×10^{21}	8
HT9-0.5wt%^{60}Ni	9×10^{21}	10	4×10^{21}	9
HT9-1.4wt%^{60}Ni	5×10^{21}	16	2×10^{21}	10

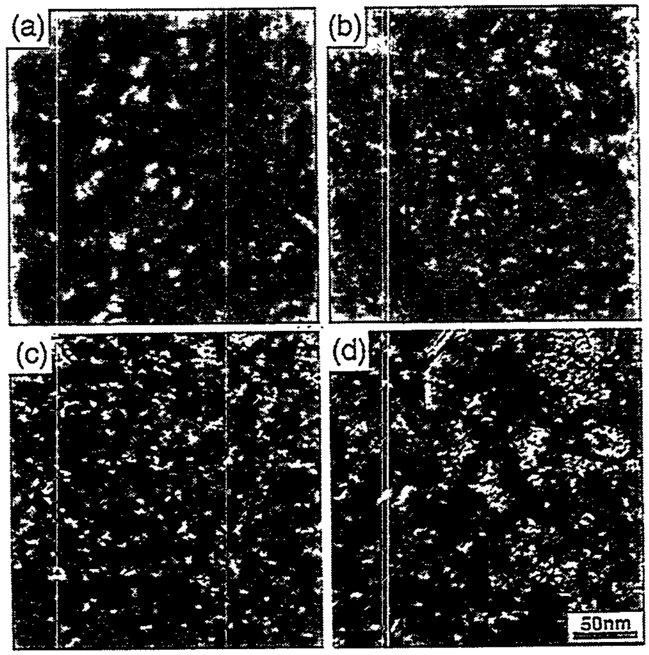

Figure 1 Dislocation segments and loops in (a) HT9-std., (b) HT9-1.4wt%^{58}Ni, (c) HT9-0.5wt%^{60}Ni and (d) HT9-1.4wt%^{60}Ni after irradiation at 400°C to 7.4 dpa using the diffraction conditions: g=110, (g,4g).

3.2 Cavities

Cavities were not observed in any of the alloys irradiated at 400°C to 7.4 dpa in HFIR. This suggests that the irradiation dose in this study was not sufficient to generate visible cavities in these steels.

3.3 Precipitates

Before irradiation, the alloys used in this study include $M_{23}C_6$ precipitates on grain boundaries with the number density and the mean diameter of about $6x10^{19}$ m^{-3} and 75 nm, respectively. The irradiation produced precipitates in the matrix and/or along dislocation loops in all alloys. The spacing of moiré fringes was used to identifiy two of the irradiation-produced precipitates, which were identified as $M_6C(\eta)$-type carbides and M_2X phase. Figures 2 and 3 show the irradiation-induced $M_6C(\eta)$-type carbides in the alloys and M_2X phase in the HT9-1.4wt%^{60}Ni alloy after irradiation at 400°C to 7.4 dpa, respectively. Precipitation of a Cr-rich $M_6C(\eta)$ has been observed in a number of 8-12Cr steels that contain > 0.3wt% Ni during FBR (Fast Breeder Reactor) and HFIR irradiation at about 400°C [13-16]. The M_2X phase was observed in 9Cr-1MoVNb-2Ni and 12Cr-1MoVW steels irradiated in HFIR at 500°C and in 9Cr-1MoVNb steel irradiated in FFTF (Fast Flux Test Facility) at 407°C [13]. XEDS compositional analysis has shown that this phase is composed of mainly Cr and N [13,14]. In addition, another type of precipitate was found along dislocation loops without moiré fringes, which was tentatively identified as α'-phase, which is a Cr-rich body-centered cubic (bcc) ferrite phase. A high density (> $x10^{22}$ m^{-3}) of α' was reported to occer in HT9 steel irradiated in the FFTF at 420°C [17]. In the present study, the M_2X phase was observed only in HT9-1.4wt%^{60}Ni alloy, while the $M_6C(\eta)$ carbides and α'-phase were found along dislocation loops in all alloys, as shown in Figure 2. The number density of $M_6C(\eta)$ carbides and α'-phase in HT9-1.4wt%^{60}Ni alloy were lower than that in the other alloys. As mentioned in section 3.1, the HT9-1.4wt%^{60}Ni alloy showed a lower number density of dislocation loops than that in the other alloys. This results suggests that dislocation loops act as sites of Cr segregation during irradiation and play important roles in the precipitation behavior in martensitic steels. Table 4 summarizes the quantitative results of precipitates.

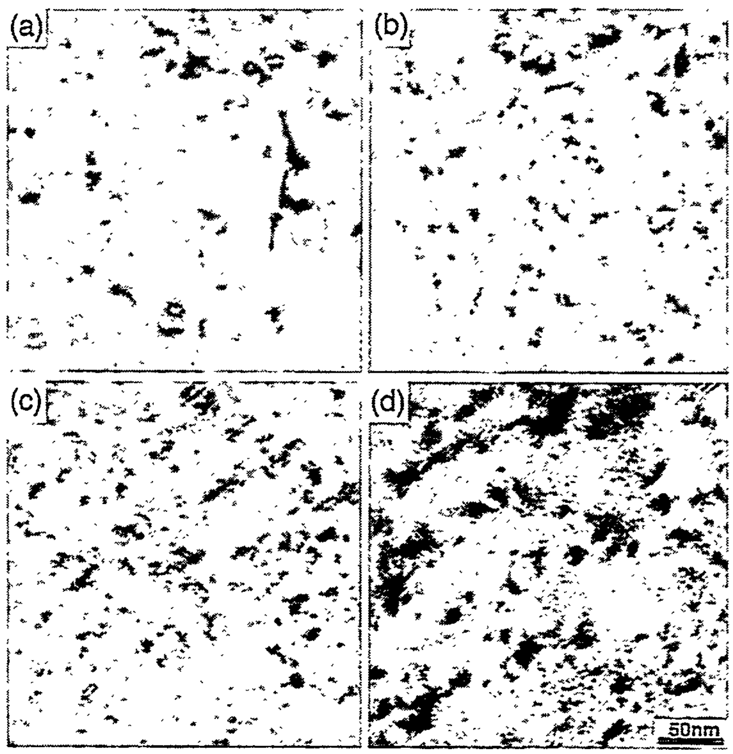

Figure 2 Irradiation-induced precipitates in (a) HT9-std., (b) HT9-1.4wt%^{58}Ni, (c) HT9-0.5wt%^{60}Ni and (d) HT9-1.4wt%^{60}Ni after irradiation at 400°C to 7.4 dpa

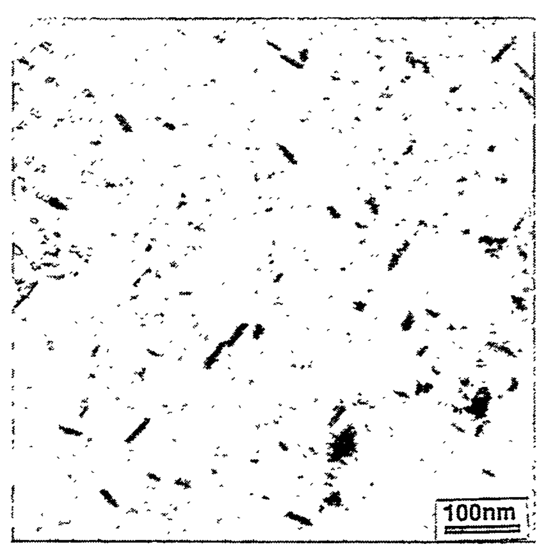

Figure 3 Irradiation-induced M_2X phase in the HT9-1.4wt%^{60}Ni alloy after irradiation at 400°C to 7.4 dpa.

Table 4. Summary of precipitates in the alloys after irradiation at 400°C to 7.4 dpa.

Steel	$M_{23}C_6$ Mean Size (nm)	$M_{23}C_6$ Number Density (m^{-3})	$M_6C(\eta)$ Mean Size (nm)	$M_6C(\eta)$ Number Density (m^{-3})	α' Mean Size (nm)	α' Number Density (m^{-3})	M_2X Mean Size (nm)	M_2X Number Density (m^{-3})
HT9-std.	75	$6x10^{19}$	6	$2x10^{21}$	4	$4x10^{21}$	-	-
HT9-1.4wt%^{58}Ni	75	$6x10^{19}$	7	$2x10^{21}$	4	$3x10^{21}$	-	-
HT9-0.5wt%^{60}Ni	75	$6x10^{19}$	6	$2x10^{21}$	4	$3x10^{21}$	-	-
HT9-1.4wt%^{60}Ni	75	$6x10^{19}$	10	$1x10^{21}$	5	$2x10^{21}$	30	$1x10^{21}$

FUTURE WORK

The investigation of isotopically-tailored martensitic steels irradiated at 400°C to about 18 dpa in HFIR will be carried out to clarify the effect of helium atoms and Ni on the formation of cavities and the microstructural development.

ACKNOWLEDGMENTS

The authors are grateful to Drs. R.L. Klueh, S.J. Zinkle and A.F. Rowcliffe for their helpful discussions. They also would like to thank L.T. Gibson and A.T. Fisher for preparation of specimens for microstructural examination, and J.J. Duff and members of hot laboratory in Oak Ridge National Laboratory for technical support. This research was supported in part by an appointment to the Oak Ridge National Laboratory Postdoctoral Research Associates Program administered jointly by the Oak Ridge Institute for Science and Education and Oak Ridge National Laboratory, and sponsored by the Office of Fusion Energy Sciences, U.S. Department of Energy, under contact DE-AC05-96 OR22464 with Lockheed Martin Energy Research Corp., and the Japan Atomic Energy Research Institute.

REFERENCES

1) R.L. Klueh, K. Ehrlich, and F Abe, J. Nucl. Mater. **191-194** (1992) 116.
2) R.L.Simon, DAFS Quarterly Progress Report, DOE/ER0046/12, p. 37, 1983
3) L.K. Mansur et al, J. Nucl. Mater. **139** (1986) 228
4) G.R. Odette, J. Nucl. Mater. **141-143** (1986) 1011
5) D.S. Gelles, Fusion Materials Semiannual Progress Report for Period Ending June 30 1996, DOE/ER-0313/20, 1996, p. 199
6) J.E. Pawel and R.L. Senn, "Status of U.S./Japan Collaborative Program Phase2 HFIR Target Capsules", Fusion Reactor Materials Semiannual Report for Period Ending March 31, 1995, DOE/ER-0313/12, 1992, p. 15.
7) J.E. Pawel, A.W. Longest, R.L. Senn, K. Shiba, D.W. Heatherly, and R.G. Sitterson, "Status of U.S./Japan Collaborative Program Phase2 HFIR Target and RB* Capsules", Fusion Reactor Materials Semiannual Report for Period Ending September 30, 1993, DOE/ER-0313/15, 1992, p. 3.
8) J.E. Pawel, K. E. Lenox and I. Ioka, "Status of U.S./Japan Collaborative Program Phase2 HFIR Target and RB* Capsules", Fusion Reactor Materials Semiannual Report for Period Ending March 31, 1995, DOE/ER-0313/18, 1995, p. 3.
9) L.R. Greenwood and C.A. Baldwin, "Neutron Dosimetry and Damage Calculations for The HFIR-JP-20 Irradiation", Fusion Reactor Materials Semiannual Report for Period Ending December 31, 1997, DOE/ER-0313/23, 1997, p. 305.
10) N. Yoshida, et al., J. Nucl. Mater., **155-157** (1988), 1232.
11) D.S. Gelles, Annual Progress Report for Fusion Year, (1991), 348.
12) E. Wakai et al., Proceeding of Ultra High Purity Base metals, UHPM-94, 488.

13) E.A. Little and L.P. Stoter, Effects of Radiation on Materials: 11th Conf., ASTM STP-782 (American Society for Testing and Materials, Philadelphia, 1982) p. 207.
14) P.J. Maziasz, R.L. Klueh and J.M. Vitek, J. Nucl. Mater. **141-143** (1986) 929.
15) P.J. Maziasz and R.L. Klueh, Effects of Radiation on Materials: 14th Conf., ASTM STP-1046 (American Society for Testing and Materials, Philadelphia, 1989) p. 35.
16) P.J. Maziasz, J. Nucl. Mater. **169** (1989) 95-115.
17) J.J. Kai and R.L. Klueh, J. Nucl. Mater. **230** (1996) 116-123